

# Robust Visual Representation Learning With Multi-modal Prior Knowledge For Image Classification Under Distribution Shift

Hongkuan Zhou<sup>1,2</sup>, Lavdim Halilaj<sup>1</sup>, Sebastian Monka<sup>1</sup>, Stefan Schmid<sup>1</sup>,  
Yuqicheng Zhu<sup>1,2</sup>, Bo Xiong<sup>3</sup>, Steffen Staab<sup>2,4</sup>

<sup>1</sup>Corporate Research, Robert Bosch GmbH, Renningen, Germany

<sup>2</sup>University of Stuttgart, Stuttgart, Germany

<sup>3</sup>Stanford University, California, US

<sup>4</sup>University of Southampton, Southampton, UK

hongkuan.zhou@de.bosch.com

## Abstract

Despite the remarkable success of deep neural networks (DNNs) in computer vision, they fail to remain high-performing when facing distribution shifts between training and testing data. In this paper, we propose **Knowledge-Guided Visual representation learning (KGV)** – a distribution-based learning approach leveraging multi-modal prior knowledge – to improve generalization under distribution shift. It integrates knowledge from two distinct modalities: 1) a knowledge graph (KG) with hierarchical and association relationships; and 2) generated synthetic images of visual elements semantically represented in the KG. The respective embeddings are generated from the given modalities in a common latent space, i.e., visual embeddings from original and synthetic images as well as knowledge graph embeddings (KGEs). These embeddings are aligned via a novel variant of translation-based KGE methods, where the node and relation embeddings of the KG are modeled as Gaussian distributions and translations, respectively. We claim that incorporating multi-modal prior knowledge enables more regularized learning of image representations. Thus, the models are able to better generalize across different data distributions. We evaluate KGV on different image classification tasks with major or minor distribution shifts, namely road sign classification across datasets from Germany, China, and Russia, image classification with the mini-ImageNet dataset and its variants, as well as the DVM-CAR dataset. The results demonstrate that KGV consistently exhibits higher accuracy and data efficiency across all experiments.

## Introduction

Deep neural networks (DNNs) have demonstrated outstanding performance in computer vision (CV) tasks. They achieved remarkable success by leveraging vast amounts of data and computational power. However, these models often struggle with generalization, especially when the test data distribution deviates from the training data distribution (Liang, He, and Tan 2023). This happens as machine learning theory assumes that training and test data are identically distributed. Therefore, DNNs tend to overfit to the training domain. The situation worsens under low data regimes (Adadi 2021), as DNNs are more prone to overfitting when insufficient training data exists. Figure 1a) illustrates three distinct examples of distribution shifts between train and test data, in particular the Road Sign, ImageNet and

Car domain. A DNN-based classifier applied to the testing domain will deteriorate in accuracy. This happens because the visual elements of the images vary between the train and test domains. For example, in Germany, warning signs have a white background, whereas in China, they use a yellow background. Similarly, ImageNet and Car differentiate between train and test data because of their style.

Over the years, numerous approaches have been presented to utilize prior knowledge to enhance the performance of DNNs. For instance, in the field of zero-shot learning (ZSL) (Chen et al. 2023), Wang, Ye, and Gupta (2018); Kampffmeyer et al. (2019) leverage additional information from a Knowledge Graphs (KG) to classify images of unseen classes. Li et al. (2023b) combines a knowledge-based classifier and a vision-based classifier to enhance the model’s ability to classify new categories. These methods are excepted to classify unseen classes based on the other seen classes sharing the same superclass. A concrete example is the classification of unseen zebras based on seen *horses* and *donkeys* as they both belong to the same superclass, i.e., *equus*. The prior knowledge contained in their KG pertains to the hierarchical levels of biological classification.

However, approaches that only use symbolic knowledge from the KG are limited to addressing the issue of data distribution shift as the symbolic knowledge lacks the connection to the visual domain. We hypothesize that the model’s ability to generalize can be further improved by leveraging multi-modal prior knowledge that (partially) covers new test data distributions. The multi-modal prior knowledge here indicates both a KG with hierarchical and association relations and generated synthetic images of visual elements semantically represented in the KG. To investigate this hypothesis, in this paper, we propose a novel neuro-symbolic approach, which aligns the image embeddings and knowledge graph embeddings (KGEs) in a common latent space by means of a variant of translation-based KGE method (Bordes et al. 2013). Thus, it regularizes the latent space with the guidance of the multi-modal prior knowledge to prevent the model from overfitting.

First, we capture information about the structures of objects in a KG (Hogan et al. 2021) to inform and enhance the learning process. For instance, warning signs are composed of a white triangle with a red border plus one pictographic el-

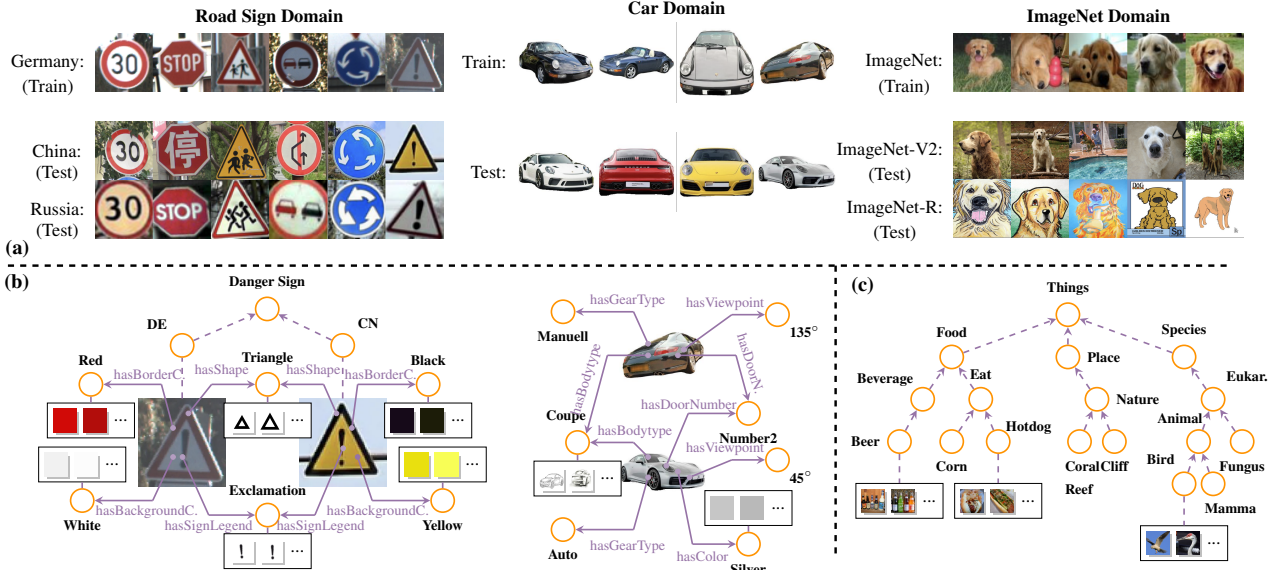


Figure 1: (a) Examples of distribution shift in road sign, ImageNet, and Car Domains. (b) Decomposition of elements w.r.t. the road signs and cars. It represents the association relations between object categories and object category elements. (c) Examples of the abstract representation of hierarchical relations in the ImageNet domain.

ement (cf. Figure 1b). Road signs in different countries share the same elements, such as the shape or the pictographic element, or both. Also, the hierarchical relations are demonstrated in Figure 1c. Combining this information, we construct a KG and develop a translation-based KGE method to map the nodes of the KG to embeddings in the latent space. An object category (e.g., ‘danger sign’) is naturally represented by its set of image vectors in the latent space. To align image and object categories, we represent the latter by a Gaussian distribution in the common latent space. Thus, the embeddings of object category elements and their relations to object categories indirectly influence the formation of categories in the latent space.

Second, for each object category element, we generate their respective synthetic images (if applicable) to augment the dataset. For instance, in the road sign domain, these elements are shape, color, and legend within the sign. These images are considered as visual prior knowledge of the object categories defined in the KG. Therefore, in this paper, the prior knowledge we used has two distinct modalities: 1) the factual knowledge across different data distributions represented in a KG, and 2) generated synthetic images of object category elements aligned with their semantic representation in the KG.

We evaluate the performance of our approach under distribution shifts and low data regimes in the context of image classification. To represent the prior knowledge, we construct three targeted KGs for the domains of Road Sign Recognition, Car Recognition, and ImageNet. Our experimental results show that KGV outperforms the image classification baselines in all experiments. Additionally, we found that our method is more data-efficient. Our main contributions are summarized as follows:

- We propose our KGV method, an end-to-end neuro-

symbolic approach that uses multi-modal prior knowledge to regularize the latent space and thus enhance the generalization ability under data distribution shift.

- We developed a new variant of translation-based KGE to align the embeddings of images and the KG in a common embedding space, where the nodes and predicates in the KG are represented as *Gaussian distributions* and *translations*, respectively.
- We evaluate KGV on various image classification datasets, namely road sign datasets, mini-ImageNet and its variants, as well as the DVM-CAR datasets. The results illustrate a notable improvement under distribution shift: 4.4% and 4.1% on average in the ImageNet and Road Sign Recognition domains. Moreover, our method improves the SOTA results on the DVM-CAR dataset and shows significant improvements on data efficiency in low data regimes.
- We analyse whether KGV can be adapted to the SOTA vision foundation models like CLIP and DINOv2. The results indicate that integrating KGV, CLIP and DINOv2 exhibit a better performance across various datasets. The code base is available at <https://anonymous.4open.science/r/kgv-D68F/>.

## Preliminaries

### Visual Embeddings

A visual encoder network  $f_\phi(\cdot) : \mathcal{I} \rightarrow \mathbb{R}^d$  with parameters of  $\phi$  maps images in image space  $\mathcal{I}$  to a visual embeddings  $z^I \in \mathbb{R}^d$ , where  $d$  is the dimension of the latent space. This function is typically realized through a series of transformations involving neural networks, particularly convolution-based models (He et al. 2015a), or Transformer-based models (Dosovitskiy et al. 2021; Carion et al. 2020).

## Knowledge Graph Embeddings

KG stores factual information of real-world entities and their relationships in triple format  $\langle head, predicate, tail \rangle$ . Knowledge graph embedding (KGE) aims to represent entities and predicates in KG into low-dimensional vectors while preserving their semantic and structural information.

Formally, we define a KG as  $\mathcal{G} \subseteq \mathcal{E} \times \mathcal{R} \times \mathcal{E}$  over a set  $\mathcal{E}$  of entities and a set  $\mathcal{R}$  of predicates. A KGE model maps entities and predicates into  $d$ -dimensional embedding  $M_\theta : \mathcal{E} \cup \mathcal{R} \rightarrow \mathbb{R}^d$ . We denote  $\langle h, r, t \rangle$  as a triple in  $\mathcal{G}$ . A score function  $s(\mathbf{h}, \mathbf{r}, \mathbf{t})$  is defined on the embeddings of a triple, which should assign higher scores to positive triples, i.e., true facts in the KG, and lower scores to negative triples, i.e., corrupted triples, generated by randomly replacing the head or tail entity in an observed triple with a random entity sampled from  $\mathcal{E}$ . The parameter  $\theta$  is learned by minimizing cross-entropy loss (Bordes et al. 2013) or margin-based loss (Sun et al. 2019).

## Few-shot Learning

A classifier  $f : x \rightarrow y$  is initially trained with a set of labeled training samples  $\mathcal{D}_{\text{tr}} = \{(x, y) | x \in \mathcal{X}, y \in \mathcal{Y}\}$ . Few-shot learning focuses on a common scenario called  $N$ -way,  $K$ -shot learning. Given a set of  $K$  labeled examples for each of  $N$  different classes  $\mathcal{D}_{\text{few}} = \{(x, y) | x \in \mathcal{X}'_{\text{few}}, y \in \mathcal{Y}'\}$ , where  $|\mathcal{Y}'| = N$  and  $\forall y_0 \in \mathcal{Y}', |\{(x, y) \in \mathcal{D}_{\text{few}} | y = y_0\}| = K$ , in the target dataset, this classifier is able to correctly predict the labels of samples in the full target dataset  $\mathcal{D}_{\text{full}} = \{(x, y) | x \in \mathcal{X}'_{\text{full}}, y \in \mathcal{Y}'\}$ , with  $(\mathcal{X} \cup \mathcal{X}'_{\text{few}}) \cap \mathcal{X}'_{\text{full}} = \emptyset$ .

## Related Work

### Use Prior Knowledge for Learning Tasks

Implicit prior knowledge in pre-trained models like CLIP (Radford et al. 2021) and DINOv2 (Oquab et al. 2024) can be leveraged by continuing to fine-tune them. Including explicit knowledge from KGs can also enhance model’s ability in visual or textual tasks (Monka, Halilaj, and Rettinger 2022b). Some approaches (Annervaz, Chowdhury, and Dukkupati 2018; Bosselut et al. 2019; Liu et al. 2020) leverage KGs to enhance language models with better reasoning ability. In the field of computer vision, KGs also play an important role. Li et al. (2023a) introduce a KG that includes inter-class relationships to the visual-language model, yielding a more effective classifier for downstream tasks. Some approaches (Zareian, Karaman, and Chang 2020; Yu et al. 2021) build scene graphs to enhance their models’ performance. There also exist some approaches use extra information in the KG to perform zero-shot learning tasks (Wang, Ye, and Gupta 2018; Kampffmeyer et al. 2019; Roy et al. 2020) or few-shot learning tasks (Li et al. 2023c; Tseng et al. 2020).

In the field of symbolic AI, some approaches include textual information (Nayyeri et al. 2023), or multi-modal information (Chen et al. 2022; Liang et al. 2023), to increase the knowledge graph reasoning ability. They combine the structured information from KGs, visual information, and textual information with transformer-based approaches. These works prove that including visual or textual information or

both is helpful for knowledge graph based reasoning and knowledge graph completion.

## Integrate Knowledge Graphs with Other Modalities

Two primary approaches are recognized in the literature to encapsulate the methodologies for integrating heterogeneous information from KGs with other modalities, such as visual and textual information. The first category (Chen et al. 2022; Liang et al. 2023; Mousselly-Sergieh et al. 2018) involves merging structural data derived from KGs — typically obtained via Graph Neural Networks (GNNs)—through the utilization of cross-attention mechanisms as employed in Transformer models. The second category (Li et al. 2023a; Monka et al. 2021; Monka, Halilaj, and Rettinger 2022a) entails aligning KGEs with visual or textual embeddings in one common space by contrastive learning (Radford et al. 2021).

In this paper, we propose a novel approach that leverages the multi-modal prior knowledge from both, a KG and synthetic images generated based on visual features that are semantically represented in the KG, in order to boost the model’s ability to generalize under data distribution shifts. Our approach aligns KGEs and visual embeddings in the *same* latent space using a new variant of translation-based KGE methods, where the nodes and relations are represented as *Gaussian distributions* and *translations*, respectively, to model the structured information in the KG within the latent space. Existing translation-based KGE methods typically represent entities and predicates with vector embeddings (Bordes et al. 2013; Wang et al. 2014; Lin et al. 2015; Socher et al. 2013). The authors (He et al. 2015b; Xiao et al. 2015) take the uncertainty of entities and predicates into account and represent them by probability distributions.

## Methodology

### Overview

We propose KGV, an approach to address the limitations of the deep learning solutions for supervised image classification and few-shot learning w.r.t. to the distribution shifts. The core idea of KGV is the inclusion of multi-modal prior knowledge coming from two different modalities: 1) domain knowledge - captured in a semantic KG; and 2) synthetic images - generated for object category elements. We encode the node and relation information from the KG and images as KGEs  $(\mathbf{r}, \mathbf{t})$  and image embeddings  $\mathbf{z}^I$  into one latent space and align them via a variant of translation-based KGE method. Here, we represent the object categories in KG as Gaussian embeddings in the latent space, and we assume each image embedding should follow the distribution of its corresponding category distribution. It extends the contrastive learning, as seen in SupCon (Khosla et al. 2020) and CLIP (Radford et al. 2021), which focuses solely on similarity and dissimilarity, by incorporating the capability to model additional individual relationships between entities.

Our approach is designed end-to-end by adding the regularization loss and cross-entropy loss together to train the network. The regularization loss aligns the KG embedding

and the visual embedding. The cross-entropy loss is used for the image classification. The architecture of KGV is depicted in Figure 2. Our model consists of three phases: the knowledge modeling phase, the training phase, and the inference phase. Here, we take the *road sign domain* as an example to describe our model.

### Knowledge Modeling

Prior knowledge used in our KGV exists in two distinct modalities. Firstly, an expert-constructed KG includes factual knowledge such as hierarchical and association relations across different data distributions. Secondly, we generate synthetic images of object category elements that are semantically represented in the KG but lack visual information in the image dataset. In the road sign recognition domain, these elements are shape, color, and the sign legend.

**Knowledge Graph Construction:** We construct a KG to represent object categories, object category elements, and the relationships between an object category and its elements based on domain knowledge. At the top level, there are two different categories: *road sign* and *road sign feature*. The *road sign* category comprises more sub-categories: *informative*, *prohibitory*, *mandatory*, and *warning*. Further, we define dedicated classes, such as Germany, China, and Russia, to model various country versions of the road signs. The *road sign feature* category contains sub-categories of *shape*, *color*, and *legend within the sign*. An illustration of hierarchical relations is demonstrated in the appendix. Besides the hierarchical information, the KG also contains four association relations. They are ‘has the shape of’, ‘has the sign legend of’, ‘has the background color of’, and ‘has the border color of’. For instance, as Figure 1b shows, the danger sign has the shape of a triangle and has the sign legend of the exclamation mark.

**Synthetic images of object category elements:** We generate synthetic images of object category elements such as shapes and colors, which is treated as visual prior knowledge. In our setting, images of different colors are generated by randomly selecting an image within the color range corresponding to the popular color definition. The images of shapes are generated by alternating on the thickness, size, and location on the canvas. The images of sign legends are extracted from standard road signs, then randomly resized and positioned at various locations on the canvas. These synthetic images are then added to the road sign dataset and trained together with those road sign images. All types of synthetic images can be seen in the appendix.

### Training

Our training loss comprises two components: the regularization loss, which is used to align the image embeddings with the KGEs, and the cross-entropy loss, which is employed for classification purposes. The regularization loss is specifically formulated to maximize the score function value for positive triplets and minimize it for negative triplets. In the following subsections, we first delineate the image, node, and relation embeddings. Subsequently, we elucidate the methodology for constructing triplets of embeddings and the

process for masking the positive and negative triplets. Next, we introduce the design of the score function for triplets. Finally, we provide a summary of the overall loss function.

**Embeddings:** Each image is provided as input into the image encoder to obtain the respective image embedding  $z^I \in \mathbb{R}^d$  in the latent space, where  $d$  is the size of the dimension. The relations from KG connecting object categories, their elements and their respective images are encoded and stored in the relation lookup table, which is represented as a list of embeddings  $[z_0^r, z_1^r, \dots, z_{N_r}^r]$ , where each  $z_i^r$  is the  $i$ -th relation vector embedding with the size of  $d$ . Note that the 0-th relation represents the inclusion relation demonstrated with purple dashed arrows as illustrated in Figure 2. The hierarchy of road signs is preserved in the KG. For instance, the images of the danger signs in Germany belong to the German danger sign category, and they also belong to the danger sign category, warning sign category, and road sign category. We use  $z_0^r$  to represent all these inclusion relations. In terms of the other  $N_r$  relations, if one node  $h$  has one relation with another node  $t$ , then all the sub-category nodes of  $h$  have such relation with the node  $t$ . For example, all warning signs have a triangle shape, including their sub-categories like danger and danger animal. The node lookup table is represented as a list of embeddings  $[z_1^o, z_2^o, \dots, z_{N_o}^o]$ , where each  $z_j^o$  denotes the  $j$ -th embedding.  $N_o$  is the total number of nodes in the KG. The node embeddings are considered as Gaussian embeddings  $z_j^o = (\mu_j, \Sigma_j)$ , where  $\mu_j$  and  $\Sigma_j$  are the mean and variance of the Gaussian distribution. Note that nodes, their relations, and respective images are embedded in the same latent space.

**Positive and Negative Triplets of Embeddings:** Following the close world assumption in the context of KG, any triplet not explicitly defined in the KG is considered to be a negative one. Since  $N_o$  nodes and  $N_r + 1$  relations exist in the KG, for each image embedding  $z^I$ ,  $(N_r + 1) \times N_o$  triplets with the embedding form of  $\langle z^I, z_i^r, z_j^o \rangle$  can be created. The positive triplets represent the defined information in the KG about the given image. To mask all the positive triplets and negative triplets for one given image, we construct a tensor  $M \in [0, 1]^{(N_r+1) \times N_o}$ :

$$M_{ij} = \begin{cases} 1 & \text{if } \langle e_{node(y)}, r_i, e_j \rangle \in \mathcal{G} \\ 1 & \text{if } r_i = \text{instanceOf} \wedge j = node(y) \\ 0 & \text{otherwise} \end{cases} \quad (1)$$

where  $e_j$  represents the  $j$ -th element in entity set  $\mathcal{E}$ .  $r_i$  is the  $i$ -th element in the relation set  $\mathcal{R}$ .  $\mathcal{G}$  represents the triplet stored in the KG.  $y$  is the class label of the given image.  $node(\cdot)$  indicates the mapping function connecting the class id of the image to the corresponding node id in the KG. As Figure 2 shows, positive triplets are marked with green color, whereas negative triplets are marked with white color.

**Score Function Design:** For a given triplet  $\langle z^I, z_i^r, z_j^o \rangle$ , we design the score function in translation-based manner which means  $z^I + z_i^r \approx z_j^o$ . In this paper, we represent image embeddings and relation embeddings as vector embeddings. The node embeddings are considered as Gaussian



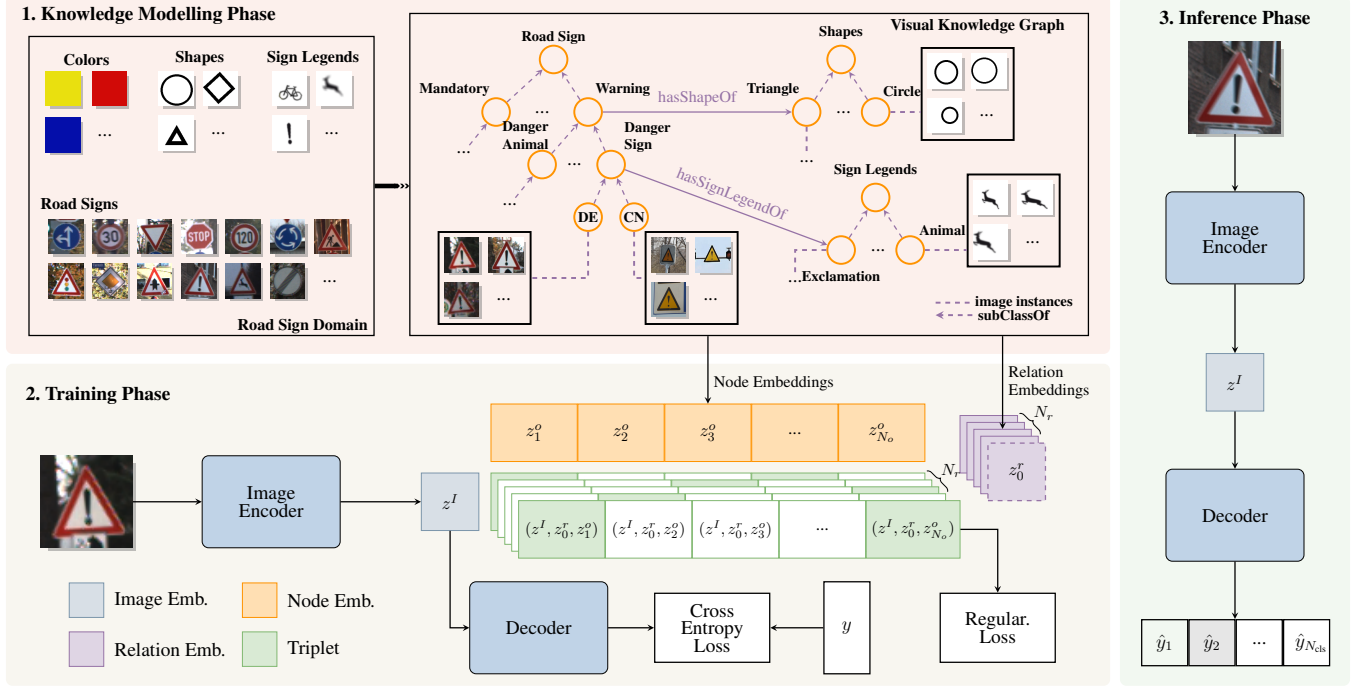


Figure 2: The KGV architecture – Our approach consists of three phases, namely knowledge modeling, training, and inference. **Knowledge modeling phase:** We create a knowledge graph based on prior domain knowledge. Also, synthetic images are generated for object categories (e.g., shapes and colors) that are semantically represented in the knowledge graph but lack visual information in the dataset. **Training phase:** The neural network is fed with both synthetic and real-world images and trained end-to-end by adding the regularization loss and cross-entropy loss together as a total loss for optimization. The image embeddings  $z^I$  and knowledge graph embeddings  $z_i^o, z_j^r$  are aligned by minimizing the regularization loss. The Cross-entropy loss is used to classify images based on their image embedding representation. **Inference phase:** The classification task is completed by selecting the class with the highest possibility based on the output of the decoder.

embeddings  $z_j^o = (\mu_j, \Sigma_j)$  to better handle the inclusion relationship between the image embedding and the node embedding, where  $\mu_j$  and  $\Sigma_j$  are the mean and variance of the Gaussian distribution. The intuition behind this is that each node in the KG contains various image instances. Thus, it is more reasonable to model the node embedding as Gaussian since each node represents a cluster of image vector embeddings. The score function can be defined as:

$$s(z^I, z_i^r, z_j^o) = \mathcal{N}(z^I + z_i^r; \mu_j, \Sigma_j) \quad (2)$$

where  $\mathcal{N}(z^I + z_i^r; \mu_j, \Sigma_j)$  denotes the possibility density of the vector  $z^I + z_i^r$  under the Gaussian distribution with parameters of  $\mu_j$  and  $\Sigma_j$ . Different score function designs are also compared in our experiments.

**Loss Functions:** During the training phase, there are two losses to minimize. The first one is the cross-entropy loss  $\mathcal{L}_{CE}(\hat{y}, y)$  to classify the images to their corresponding classes, where  $\hat{y}$  is the predicted possibility of classes and  $y$  is the ground truth class label in the form of one-hot-key.

The other loss term is the regularization loss. It aims to regularize the latent space with prior knowledge by aligning image embeddings with KG embeddings. Here, we represent the relationships from the KG in the visual latent space by optimizing the score function as defined in Equation (2). If the score function has high scores for positive triplets and low scores for negative triplets, the image embeddings and

the KGEs are then well aligned in the latent space. The regularization loss is defined as follows:

$$\mathcal{L}_{reg} = \frac{\sum_{i,j} M_{ij} \cdot S_{ij}}{\sum_{i,j} M_{ij}} + \frac{\sum_{i,j} (1 - M_{ij}) \cdot \max\{0, \epsilon - S_{ij}\}}{\sum_{i,j} 1 - M_{ij}} \quad (3)$$

where  $\mathbf{M}$  is the mask defined in Equation (1).  $\mathbf{S} \in R^{(N_r+1) \times N_o}$  and  $S_{ij} = -\log(s(z^I, z_i^r, z_j^o))$ , following the negative log likelihood form.  $\epsilon$  is the threshold score difference between positive and negative triplets. Finally, the total loss is defined by:

$$\mathcal{L} = \mathcal{L}_{CE} + \beta \mathcal{L}_{reg}, \quad (4)$$

where  $\beta$  is the hyper-parameter used to balance the cross-entropy loss term and regularization loss term.

### Inference Phase

At the inference phase, the classification task is completed by selecting the class with the highest probability based on the output of the decoder  $\hat{y}$ .

## Experiments

In this section, we first explain the datasets and the respective knowledge graphs used in our experiments. Then, we analyze the results of supervised image classification experiments under varying conditions, including data distribution

shifts, low-data regimes, and few-shot learning scenarios. The experimental details are listed in the appendix section.

## Datasets

In our experiments, we evaluate KGV in three domains, namely Road Sign, Car Recognition, and ImageNet.

- **Road Sign Recognition:** It includes three commonly used road sign datasets from Germany, China, and Russia: German Traffic Sign Recognition Benchmark (GTSRB) from Stallkamp et al. (2011), Chinese Traffic Sign Dataset (CTSD) from Yang et al. (2015), and Russian Traffic Sign Images Dataset (RTSD) from Shakhuro and Konouchine (2016).
- **Car Recognition:** We use the Deep Visual Marketing Car (DVM-CAR) dataset (Huang et al. 2021) which contains *millions* of car images captured under various conditions and viewpoints, accompanied by detailed annotations including car make, seat count, door count, color, body type and etc. The primary task here is to classify the car model based on the provided image.
- **ImageNet:** In this domain, we use the well-known mini-ImageNet (Vinyals et al. 2016), ImageNet-Sketch (Wang et al. 2019), ImageNetV2 (Recht et al. 2019), ImageNet-R (Hendrycks et al. 2021a), and ImageNet-A (Hendrycks et al. 2021b) for our experiments.

## Knowledge Graphs

**Road Sign Recognition Knowledge Graph:** The constructed knowledge graph contains 202 nodes and 5 relations. The 5 relations we include are ‘has the background color of’, ‘has the border color of’, ‘has the sign legend of’, ‘has the shape of’, ‘instance/subclass’.

**Car Recognition Knowledge Graph:** The knowledge graph for the DVM-CAR contains 386 nodes and 9 relations. These relations are ‘hasBodyType’, ‘hasColor’, ‘hasDoorNo’, ‘hasFuelType’, ‘hasGearbox’, ‘hasMaker’, ‘hasSeatNo’, ‘hasViewpoint’, ‘instanceOf’. The dataset includes annotations such as body type, color, and car make for each image, provided in tabular form. We construct a KG by defining the ontology and triplets based on the tabular annotations. We generate pure color images using the same method as in the road sign domain to serve as visual prior knowledge. Further, we collect sketch images representing body types such as SUV, Coupe, and Limousine. Examples of these body type sketches are provided in the appendix.

**ImageNet Knowledge Graph:** We leverage WordNet (Miller 1995; Fellbaum 2010), which is a lexical database containing nouns, verbs, adjectives, and adverbs of the English language structured into respective synsets and create the subset of Wordnet by extracting the respective synsets of each label from the mini-ImageNet dataset. These synsets are grouped based on the lexical domain they pertain to, e.g., animal, artifact, or food; thus, we get hierarchical relations between the classes in the mini-ImageNet from the WordNet. We also include two association relations: ‘has color’ and ‘has sketch’. We use the generated pure color images in the domain of road signs and the sketch images

from ImageNet-Sketch. It contains 234 nodes and 3 relations: ‘subclass/instance of’, ‘has color’ and ‘has sketch’.

## Results

We conducted a number of supervised image classification experiments with major and minor distribution shifts and low data regimes. Further, we evaluated the model’s adaptability on few-shot learning experiments using data with altered distributions.

Prior Know.			Model	GTSRB (43)	CTSD (25)	RTSD (36)
Imp.	KG	VP				
×	×	×	ResNet50	98.9% (+0.4%)	71.5% (+3.3%)	72.8% (+7.3%)
✓	×	×	CLIP+LP	77.2% (+22.1%)	73.5% (+1.3%)	60.0% (+20.1%)
✓	×	×	DINOv2+LP	78.7% (+20.6%)	28.9% (+49.5%)	59.9% (+20.2%)
×	✓	×	DGP	99.0% (+0.3%)	72.0% (+2.8%)	73.5% (+6.6%)
×	✓	✓	GCNZ	99.1% (+0.2%)	71.1% (+3.7%)	74.9% (+5.2%)
×	✓	✓	KGV (ours)	<b>99.3%</b>	<b>74.8%</b>	<b>80.1%</b>
×	×	✓	ResNet50 <sup>+</sup>	98.9%	71.8%	72.7%
×	✓	×	KGV <sup>−</sup>	99.0%	72.5%	74.0%

Table 1: Road Sign Classification Accuracy. Evaluation results with the test data of GTSRB and the full data of CTSD and RTSD. Imp. refers to the implicit prior knowledge in pre-trained models, while KG indicates explicit prior knowledge from the knowledge graph. VP denotes the visual prior associated with object category elements.






Classes	Images	ResNet50		KGV	
		Precision	Recall	Precision	Recall
STOP		21.3%	74.6%	<b>48.2%</b>	<b>98.1%</b>
Danger		0.0%	0.0%	<b>10.8%</b>	<b>14.9%</b>
BendLeft		0.0%	0.0%	<b>3.5%</b>	<b>32.1%</b>
PedestrianCross		0.0%	0.0%	<b>9.1%</b>	<b>65.6%</b>
SchoolCross		0.0%	0.0%	<b>20.1%</b>	<b>25.4%</b>

Table 2: Precision and recall of representative classes for road sign classification when training with 43 classes data of GTSRB and testing with shared 25 classes data of CTSD.

### Image Classification under Data Distribution Shifts:

We train our KGV model and ResNet50 with the GTSRB dataset plus generated synthetic images from scratch. It is then evaluated with test data of GTSRB with 43 classes, the full data of CTSD with 25 shared classes, and the full data of RTSD with 36 shared classes. The shared classes here indicate those classes that both datasets contain. As shown in Table 1, all models’ accuracy drops in distribution shift scenarios, i.e., from Germany to China or Russia. By incorporating the multi-modal prior knowledge, our KGV reaches an obvious improvement compared to other baselines, such as DGP (Kampffmeyer et al. 2019) and GCNZ (Wang, Ye, and Gupta 2018). These two are ZSL baselines, which leverage additional information from KGs. Fine-tuning pretrained CLIP and DINOv2 with linear probing does not work well in road sign domain. ‘ResNet50<sup>+</sup>’ refers to the model trained with additional synthetic images and ‘KGV<sup>−</sup>’ denotes the model trained without synthetic images. As the experiments indicate, our KGV model surpasses the ResNet50 baseline by

3.3% in CTSD and 7.3% in RTSD. We also observe that the inclusion of synthetic images featuring elements of object categories, such as colors and shapes, enhances the generalization ability of the KGV models across various data distributions. On the other hand, it does not have a significant effect on the ResNet50’s performance. The precision and recall for a subset of classes in CTSD are presented in Table 2. As the table illustrates, the ResNet50 fails to classify specific classes, including danger signs, pedestrian crossing, etc. In contrast, the KGV models exhibit significant improvements in both precision and recall.



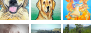

Datasets	Samples	ResNet50	KGNN	ResNet50 <sup>+</sup>	KGV	CLIP+LP	DINOv2+LP
Mini-ImageNet		62.6% +4.2%	66.2% +0.6%	59.6% +7.2%	<b>66.8%</b>	87.0%	94.9%
ImageNetV2		50.5% +2.2%	52.5% +0.2%	48.0% +4.7%	<b>52.7%</b>	87.5%	91.5%
ImageNet-R		25.5% +15.9%	30.0% +11.4%	36.9% +4.5%	<b>41.4%</b>	90.6%	86.1%
ImageNet-A		4.7% +2.1%	5.3% +1.5%	5.0% +1.8%	<b>6.8%</b>	53.8%	84.5%

Table 3: Classification Accuracy in the ImageNet Domain. ResNet50<sup>+</sup> refers to the ResNet50 model trained with additional visual prior images.

We also evaluate our method in the ImageNet domain. The baselines we choose are ResNet50, DINOv2, CLIP, and KGNN (Monka, Halilaj, and Rettinger 2022a). KGNN represents another approach to integrate prior knowledge into learning pipeline through pre-training. Our model outperforms the baselines KGNN and ResNet50 in all these datasets. As Table 3 shows, these baselines fail, particularly when the distribution shift increases (from Mini-ImageNet to ImageNetV2, ImageNet-R, and ImageNet-A). Our KGV suffers less when data distribution changes. We also observe that incorporating visual priors without the guidance of symbolic knowledge from the KG may negatively impact performance in scenarios where the difference between training and test distributions is minimal. Compared to ResNet50, ResNet50<sup>+</sup>’s performance decreases from 62.6% to 59.6% on mini-ImageNet and from 50.5% to 48.0% on ImageNetV2. We believe this is due to the visual priors altering the distribution of the training data, making it different from the test distribution. However, DINOv2 and CLIP fine-tuned with linear probing achieve better performance than our model, as they are pre-trained on massive data, including ImageNet and its variants. We conducted additional experiments by combining DINOv2 and CLIP with our approach, respectively, as described in Section .

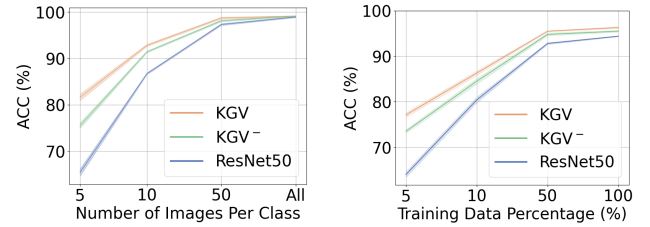
Model	SimCLR	MMCL	SupCon	ResNet50	CLIP+LP	DINOv2+LP	KGV (Ours)
ACC	88.8% +7.5%	94.4% +1.9%	93.8% +2.5%	94.3% +2.0%	65.8% +30.5%	89.3% +7.0%	<b>96.3%</b>

Table 4: Accuracy in DVM-CAR Classification.

Next, we evaluate KGV in the DVM-CAR dataset. We observe that even though the test and training data have no significant distribution shift, it still improves performance. The baselines we choose are contrastive learning approaches such as SimCLR (Chen et al. 2020) and SupCon (Khosla et al. 2020) as well as the SOTA model MMCL (Hager,

Menten, and Rueckert 2023), which combines the tabular data and image data to enhance the model’s performance through contrastive learning. Table 4 shows that our model outperforms all baselines. In the mini-ImageNet domain, KGV achieves a 4.2% performance gain compared to ResNet50.

**Performance in Low Data Regimes:** Figure 3 shows the evaluation results KGV in low data regimes. We see that our method significantly outperforms the ResNet50 baseline, particularly when the amount of training data is limited. With the increase of training data, the performance of the two models gradually converges. However, KGV consistently outperforms the baseline among all training settings. The performance of KGV<sup>-</sup> – the variant of KGV trained without synthetic images – is also shown in Figure 3. It indicates that without the visual priors, its performance drops.



(a) Road Sign Classification in GTSRB. (b) DVM-CAR Model Classification.

Figure 3: Performance under Low Data Regime. KGV<sup>-</sup> is the KGV variant trained without synthetic images.

Experiments	Models	CTSD (58 classes)	RTSD (64 classes)
One-shot	ResNet50	68.4% (+7.0%)	57.9% (+5.2%)
	KGV	<b>75.4%</b>	<b>63.1%</b>
Five-shot	ResNet50	98.7% (+0.2%)	81.2% (+2.3%)
	KGV	<b>98.9%</b>	<b>83.5%</b>

Table 5: One-shot and five-shot learning results in the datasets of CTSD and RTSD are demonstrated in the table.

**Few-shot Learning:** We conduct our few-shot learning tasks in the domain of road sign recognition. We first train the models with the GTSRB dataset. Then, we keep the encoder network and replace the decoder to fit the right class dimension in the target dataset. The new decoder is randomly initialized. The models are retrained with different amounts of labeled target data in the CTSD or the RTSD. We perform one-shot and five-shot learning experiments. One-shot learning involves using just one image per class from the target dataset for retraining. Similarly, five-shot learning uses five images per class in the target dataset for retraining. As Table 5 shows that KGV achieves 7.0% performance gain in the CTSD dataset and 5.2% in the RTSD dataset in one-shot learning. In a five-shot learning setting, the KGV model achieves 0.2 % improvement in CTSD and 2.3% improvement in RTSD.

Prior Knowledge Imp.	KG	Model	Road Sign Domain			ImageNet Domain				Car Domain
			GTSRB	CTSD	RTSD	Mini-ImageNet	ImageNetV2	ImageNet-R	ImageNet-A	DVM-CAR
✓	✓	P-ResNet50+KGV	99.5%	74.5%	79.8%	81.8%	62.4%	56.6%	6.4%	97.0%
✓	✗	P-ResNet50	99.3% (+0.2%)	73.1% (+1.4%)	72.5% (+7.3%)	75.0% (+6.8%)	61.3% (+1.1%)	51.6% (+5.0%)	4.4% (+2.0%)	96.2% (+0.8%)
✓	✓	DINOv2+KGV	79.1%	31.2%	62.4%	95.4%	92.4%	87.0%	85.4%	92.8%
✓	✗	DINOv2+LP	78.7% (+0.4%)	28.9% (+2.3%)	59.9% (+2.5%)	94.9% (+0.6%)	91.5% (+0.9%)	86.1% (+0.9%)	84.3% (+1.1%)	89.3% (+3.5%)
✓	✓	CLIP-I+KGV	89.3%	73.0%	67.8%	90.1%	89.1%	83.2%	50.1%	90.5%
✓	✗	CLIP-I+LP	89.1% (+0.2%)	73.5% (-0.5%)	60.0% (+7.8%)	89.7% (+0.4%)	88.9% (+0.2%)	82.9% (+0.3%)	49.6% (+0.5%)	89.2% (+1.3%)

Table 6: Pre-trained ResNet50, DINOv2 (1B), and CLIP Image encoder, which are denoted as P-ResNet50, DINOv2, and CLIP-I, are used for our experiments. LP represents linear probing for fine-tuning. Our KGV’s encoder is replaced by one of these pre-trained image encoders denoted by X+KGV.

Model	Road Sign Domain			ImageNet Domain				Car Domain
	GTSRB	CTSD	RTSD	Mini-ImageNet	ImageNetV2	ImageNet-R	ImageNet-A	DVM-CAR
KGV	99.3%	<b>74.8%</b>	<b>80.1%</b>	<b>66.8%</b>	<b>52.7%</b>	<b>41.4%</b>	<b>6.8%</b>	<b>96.3%</b>
KGV w/o Gaussian Emb.	<b>99.4%</b> (-0.1%)	74.7% (+0.1%)	79.9% (+0.2%)	61.2% (+5.6%)	49.0% (+3.7%)	37.8% (+3.6%)	4.8% (+2.0%)	96.3% (+0.0%)
KGV w/ TransH	99.3% (0.0%)	73.5% (+1.3%)	79.3% (+0.0%)	61.8% (+5.0%)	48.2% (+4.5%)	38.6% (+2.8%)	5.5% (+1.3%)	95.8% (+0.5%)
KGV w/ DistMult	99.2% (+0.1%)	73.7% (+1.1%)	75.6% (+5.4%)	60.5% (+6.3%)	47.6% (+5.1%)	37.5% (+3.1%)	4.7% (+2.1%)	95.1% (+1.2%)
KGV w/ RGCN	99.3% (+0.0%)	74.1% (+0.7%)	78.5% (+1.6%)	63.5% (+3.3%)	50.6% (+2.1%)	39.7% (+1.7%)	6.1% (+0.7%)	-

Table 7: KGV with alternative score function designs like TransH, DistMult, and replacing Gaussian embeddings with vector embeddings are listed in the table. KGV with GNN-based method like RGCN are also compared.

**Combining Implicit and Explicit Prior Knowledge** In this sub-section, we investigate if combining implicit prior knowledge from the pre-trained models and explicit multi-modal prior knowledge from KG and visual prior images can further improve our method’s performance. We conduct experiments by replacing the random initialized ResNet50 encoder with pre-trained ResNet50, DINOv2(1B), and the image encoder of CLIP. As shown in Table 6, applying our method to these pre-trained encoders consistently enhances performance across all three domains. Although DINOv2 and CLIP have already achieved strong results on the ImageNet domain, the incorporation of KGV further improves their performance. These results indicate that our method can be adapted to state-of-the-art pre-trained image encoders to further enhance their performance.

## Ablation Study

**Score Functions** Here, we compare four score function designs: (1) replacing the Gaussian-form node embedding with vector embedding (TransE), (2) using TransH’s score function, (3) adopting DistMult’s score function, and (4) incorporating R-GCN, a GNN-based method. As Table 7 shows, overall KGV performs best among all these score function designs. The performance of KGV without Gaussian embedding drops significantly in the ImageNet domain compared to other domains. This highlights the importance of using Gaussian embedding for node representation to handle inclusion relations between object categories and their respective images. The DistMult demonstrates sub-optimal performance across all three visual domains. While GNN-based method R-GCN outperform TransH and DistMult, it still does not surpass the effectiveness of our original score function design.

**Knowledge types** Here, we further analyze the impact of relations types in the KGV’s performance. We conduct ablation experiments on road sign recognition, car recognition.

As Table 8 demonstrates, in each study, one type of relation is excluded, i.e. sign legends, colors, and shapes. Our findings indicate that shape is the most critical factor in enhancing performance under the distribution shift from German to Chinese and Russian road signs. This is likely because road signs with the same semantic meaning share identical shapes in Germany, China, and Russia. Sign legends also significantly contributes to performance, while information about colors is the least impactful.

Model	CTSD	RTSD
KGV	<b>74.8%</b>	<b>80.1%</b>
KGV w/o sign legend	73.4% (+1.4%)	75.5% (+4.6%)
KGV w/o colors	73.7% (+1.1%)	77.2% (+2.9%)
KGV w/o shapes	72.8% (+2.0%)	74.7% (+5.4%)

Table 8: Classification Accuracy in the Road Sign Domain. The models are trained with 43 classes data of GTSRB and testing with shared 25 classes data of CTSD and shared 36 classes data of RTSD.

On the DVM-CAR dataset, we performed experiments in a setting with 5% training data. We observe that even with this amount of data, KGV exhibits a large performance margin compared to the baselines. As indicated in Table 9, the information about the body type is the most important factor in improving performance. Without this information, there is a significant drop of 4.0%. Additionally, prior knowledge of colors is also crucial, as the performance drops by 2.4% without color information.

We also found that non-morphometric features, such as gear type and fuel type, can also influence performance. This is likely because specific car models are often available only with certain types of gear and fuel. For instance, Tesla primarily produces electric cars, and most of them are automatic. The prior knowledge of the image viewpoint does not play a significant role.



Model	Accuracy	Model	Accuracy
KGv	<b>77.1%</b>	ResNet50	64.0% (+13.1%)
KGv w/o body type	73.1% (+4.0%)	KGv w/o color	74.7% (+2.4%)
KGv w/o viewpoint	76.2% (+0.9%)	KGv w/o non-morpho.	75.2% (+1.9%)

Table 9: Accuracy in DVM-CAR Model Classification with 5% Training Data.

## Conclusion and Future Work

In this paper, we introduce KGv, a knowledge-guided visual representation learning method that leverages multi-modal prior knowledge to improve generalization in deep learning. The multi-modal prior knowledge across data distributions in KGv helps to mitigate overfitting the training dataset, thereby enhancing the robustness of the model against data distribution shifts. We observe that modeling node embeddings of the KG as Gaussian embeddings enhances the performance of KGv to model hierarchical relations. Furthermore, our method demonstrates a strong tendency to be data efficient, i.e consistently achieves good performance in the low data regimes. Finally, we show that our KGv method can be well adapted to the SOTA visual foundation models such as DINOv2 and CLIP.

A main objective of our future work is to scale our concept to larger datasets and KGs. Additionally, we plan to explore further methods for aligning KGEs and image embeddings, and inducing information of the KG at inference time. Lastly, we will look whether incorporating additional text information will improve the performance.

## References

- Adadi, A. 2021. A survey on data-efficient algorithms in big data era. *Journal of Big Data*, 8(1): 24.
- Annervaz, K. M.; Chowdhury, S. B. R.; and Dukkupati, A. 2018. Learning beyond datasets: Knowledge Graph Augmented Neural Networks for Natural language Processing. arXiv:1802.05930.
- Bordes, A.; Usunier, N.; Garcia-Duran, A.; Weston, J.; and Yakhnenko, O. 2013. Translating Embeddings for Modeling Multi-relational Data. In Burges, C.; Bottou, L.; Welling, M.; Ghahramani, Z.; and Weinberger, K., eds., *Advances in Neural Information Processing Systems*, volume 26. Curran Associates, Inc.
- Bosselut, A.; Rashkin, H.; Sap, M.; Malaviya, C.; Celikyilmaz, A.; and Choi, Y. 2019. COMET: Commonsense Transformers for Automatic Knowledge Graph Construction. In *Proceedings of the 57th Annual Meeting of the Association for Computational Linguistics*, 4762–4779. Association for Computational Linguistics.
- Carion, N.; Massa, F.; Synnaeve, G.; Usunier, N.; Kirillov, A.; and Zagoruyko, S. 2020. End-to-End Object Detection with Transformers. arXiv:2005.12872.
- Chen, J.; Geng, Y.; Chen, Z.; Pan, J. Z.; He, Y.; Zhang, W.; Horrocks, I.; and Chen, H. 2023. Zero-shot and few-shot learning with knowledge graphs: A comprehensive survey. *Proceedings of the IEEE*.
- Chen, T.; Kornblith, S.; Norouzi, M.; and Hinton, G. 2020. A Simple Framework for Contrastive Learning of Visual Representations. In III, H. D.; and Singh, A., eds., *Proceedings of the 37th International Conference on Machine Learning*, volume 119 of *Proceedings of Machine Learning Research*, 1597–1607. PMLR.
- Chen, X.; Zhang, N.; Li, L.; Deng, S.; Tan, C.; Xu, C.; Huang, F.; Si, L.; and Chen, H. 2022. Hybrid transformer with multi-level fusion for multimodal knowledge graph completion. In *Proceedings of the 45th international ACM SIGIR conference on research and development in information retrieval*, 904–915.
- Dosovitskiy, A.; Beyer, L.; Kolesnikov, A.; Weissenborn, D.; Zhai, X.; Unterthiner, T.; Dehghani, M.; Minderer, M.; Heigold, G.; Gelly, S.; Uszkoreit, J.; and Houlsby, N. 2021. An Image is Worth 16x16 Words: Transformers for Image Recognition at Scale. arXiv:2010.11929.
- Fellbaum, C. 2010. WordNet. In *Theory and applications of ontology: computer applications*, 231–243. Springer.
- Hager, P.; Menten, M. J.; and Rueckert, D. 2023. Best of Both Worlds: Multimodal Contrastive Learning With Tabular and Imaging Data. In *Proceedings of the IEEE/CVF Conference on Computer Vision and Pattern Recognition (CVPR)*, 23924–23935.
- He, K.; Zhang, X.; Ren, S.; and Sun, J. 2015a. Deep Residual Learning for Image Recognition. *CoRR*, abs/1512.03385.
- He, S.; Liu, K.; Ji, G.; and Zhao, J. 2015b. Learning to represent knowledge graphs with gaussian embedding. In *Proceedings of the 24th ACM international conference on information and knowledge management*, 623–632.
- Hendrycks, D.; Basart, S.; Mu, N.; Kadavath, S.; Wang, F.; Dorundo, E.; Desai, R.; Zhu, T.; Parajuli, S.; Guo, M.; et al. 2021a. The many faces of robustness: A critical analysis of out-of-distribution generalization. In *Proceedings of the IEEE/CVF international conference on computer vision*, 8340–8349.
- Hendrycks, D.; Zhao, K.; Basart, S.; Steinhardt, J.; and Song, D. 2021b. Natural adversarial examples. In *Proceedings of the IEEE/CVF conference on computer vision and pattern recognition*, 15262–15271.
- Hogan, A.; Blomqvist, E.; Cochez, M.; d’Amato, C.; Melo, G. D.; Gutierrez, C.; Kirrane, S.; Gayo, J. E. L.; Navigli, R.; Neumaier, S.; et al. 2021. Knowledge graphs. *ACM Computing Surveys (Csur)*, 54(4): 1–37.
- Huang, J.; Chen, B.; Luo, L.; Yue, S.; and Ounis, I. 2021. DVM-CAR: A large-scale automotive dataset for visual marketing research and applications. *CoRR*, abs/2109.00881.
- Kampffmeyer, M.; Chen, Y.; Liang, X.; Wang, H.; Zhang, Y.; and Xing, E. P. 2019. Rethinking Knowledge Graph Propagation for Zero-Shot Learning. In *Proceedings of the IEEE/CVF Conference on Computer Vision and Pattern Recognition (CVPR)*.
- Khosla, P.; Teterwak, P.; Wang, C.; Sarna, A.; Tian, Y.; Isola, P.; Maschinot, A.; Liu, C.; and Krishnan, D. 2020. Supervised Contrastive Learning. *CoRR*, abs/2004.11362.

- Li, X.; Lian, D.; Lu, Z.; Bai, J.; Chen, Z.; and Wang, X. 2023a. GraphAdapter: Tuning Vision-Language Models With Dual Knowledge Graph. In *Advances in Neural Information Processing Systems*, volume 36, 13448–13466. Curran Associates, Inc.
- Li, Z.; Tang, H.; Peng, Z.; Qi, G.-J.; and Tang, J. 2023b. Knowledge-guided semantic transfer network for few-shot image recognition. *IEEE Transactions on Neural Networks and Learning Systems*.
- Li, Z.; Tang, H.; Peng, Z.; Qi, G.-J.; and Tang, J. 2023c. Knowledge-Guided Semantic Transfer Network for Few-Shot Image Recognition. *IEEE Transactions on Neural Networks and Learning Systems*, 1–15.
- Liang, J.; He, R.; and Tan, T.-P. 2023. A Comprehensive Survey on Test-Time Adaptation under Distribution Shifts. *ArXiv*, abs/2303.15361.
- Liang, K.; Zhou, S.; Liu, Y.; Meng, L.; Liu, M.; and Liu, X. 2023. Structure guided multi-modal pre-trained transformer for knowledge graph reasoning. *arXiv preprint arXiv:2307.03591*.
- Lin, Y.; Liu, Z.; Sun, M.; Liu, Y.; and Zhu, X. 2015. Learning entity and relation embeddings for knowledge graph completion. In *Proceedings of the AAAI conference on artificial intelligence*, volume 29.
- Liu, W.; Zhou, P.; Zhao, Z.; Wang, Z.; Ju, Q.; Deng, H.; and Wang, P. 2020. K-bert: Enabling language representation with knowledge graph. In *Proceedings of the AAAI Conference on Artificial Intelligence*, volume 34, 2901–2908.
- Miller, G. A. 1995. WordNet: a lexical database for English. *Communications of the ACM*, 38(11): 39–41.
- Monka, S.; Halilaj, L.; and Rettinger, A. 2022a. Context-Driven Visual Object Recognition Based on Knowledge Graphs. In *The Semantic Web - ISWC 2022 - 21st International Semantic Web Conference, Virtual Event, October 23-27, 2022, Proceedings*, volume 13489 of *Lecture Notes in Computer Science*, 142–160. Springer.
- Monka, S.; Halilaj, L.; and Rettinger, A. 2022b. A survey on visual transfer learning using knowledge graphs. *Semantic Web*, 13(3): 477–510.
- Monka, S.; Halilaj, L.; Schmid, S.; and Rettinger, A. 2021. Learning Visual Models Using a Knowledge Graph as a Trainer. In *The Semantic Web – ISWC 2021*, 357–373. Cham: Springer International Publishing. ISBN 978-3-030-88361-4.
- Mousselly-Sergie, H.; Botschen, T.; Gurevych, I.; and Roth, S. 2018. A multimodal translation-based approach for knowledge graph representation learning. In *Proceedings of the Seventh Joint Conference on Lexical and Computational Semantics*, 225–234.
- Nayyeri, M.; Wang, Z.; Akter, M. M.; Alam, M. M.; Rony, M. R. A. H.; Lehmann, J.; and Staab, S. 2023. Integrating Knowledge Graph embedding and pretrained Language Models in Hypercomplex Spaces. *arXiv:2208.02743*.
- Oquab, M.; Darcet, T.; Moutakanni, T.; Vo, H. V.; Szafraniec, M.; Khalidov, V.; Fernandez, P.; Haziza, D.; Massa, F.; El-Nouby, A.; Assran, M.; Ballas, N.; Galuba, W.; Howes, R.; Huang, P.; Li, S.; Misra, I.; Rabbat, M.; Sharma, V.; Synnaeve, G.; Xu, H.; Jégou, H.; Mairal, J.; Labatut, P.; Joulin, A.; and Bojanowski, P. 2024. DINOv2: Learning Robust Visual Features without Supervision. *Trans. Mach. Learn. Res.*, 2024.
- Radford, A.; Kim, J. W.; Hallacy, C.; Ramesh, A.; Goh, G.; Agarwal, S.; Sastry, G.; Askell, A.; Mishkin, P.; Clark, J.; Krueger, G.; and Sutskever, I. 2021. Learning Transferable Visual Models From Natural Language Supervision. *arXiv:2103.00020*.
- Recht, B.; Roelofs, R.; Schmidt, L.; and Shankar, V. 2019. Do imagenet classifiers generalize to imagenet? In *International conference on machine learning*, 5389–5400. PMLR.
- Roy, A.; Ghosal, D.; Cambria, E.; Majumder, N.; Mihalcea, R.; and Poria, S. 2020. Improving Zero Shot Learning Baselines with Commonsense Knowledge. *CoRR*, abs/2012.06236.
- Shakhuro, V. I.; and Konouchine, A. 2016. Russian traffic sign images dataset. *Computer optics*, 40(2): 294–300.
- Socher, R.; Chen, D.; Manning, C. D.; and Ng, A. 2013. Reasoning with neural tensor networks for knowledge base completion. *Advances in neural information processing systems*, 26.
- Stallkamp, J.; Schlipsing, M.; Salmen, J.; and Igel, C. 2011. The German Traffic Sign Recognition Benchmark: A multi-class classification competition. In *The 2011 International Joint Conference on Neural Networks*, 1453–1460.
- Sun, Z.; Deng, Z.; Nie, J.; and Tang, J. 2019. RotatE: Knowledge Graph Embedding by Relational Rotation in Complex Space. In *ICLR (Poster)*. OpenReview.net.
- Tseng, H.; Lee, H.; Huang, J.; and Yang, M. 2020. Cross-Domain Few-Shot Classification via Learned Feature-Wise Transformation. *CoRR*, abs/2001.08735.
- Vinyals, O.; Blundell, C.; Lillicrap, T.; Wierstra, D.; et al. 2016. Matching networks for one shot learning. *Advances in neural information processing systems*, 29.
- Wang, H.; Ge, S.; Lipton, Z.; and Xing, E. P. 2019. Learning Robust Global Representations by Penalizing Local Predictive Power. In Wallach, H.; Larochelle, H.; Beygelzimer, A.; d'Alché-Buc, F.; Fox, E.; and Garnett, R., eds., *Advances in Neural Information Processing Systems*, volume 32. Curran Associates, Inc.
- Wang, X.; Ye, Y.; and Gupta, A. 2018. Zero-shot recognition via semantic embeddings and knowledge graphs. In *Proceedings of the IEEE conference on computer vision and pattern recognition*, 6857–6866.
- Wang, Z.; Zhang, J.; Feng, J.; and Chen, Z. 2014. Knowledge graph embedding by translating on hyperplanes. In *Proceedings of the AAAI conference on artificial intelligence*, volume 28.
- Xiao, H.; Huang, M.; Hao, Y.; and Zhu, X. 2015. Transg: A generative mixture model for knowledge graph embedding. *arXiv preprint arXiv:1509.05488*.
- Yang, Y.; Luo, H.; Xu, H.; and Wu, F. 2015. Towards real-time traffic sign detection and classification. *IEEE Transactions on Intelligent transportation systems*, 17(7).



Yu, F.; Tang, J.; Yin, W.; Sun, Y.; Tian, H.; Wu, H.; and Wang, H. 2021. Ernie-vil: Knowledge enhanced vision-language representations through scene graphs. In *Proceedings of the AAAI conference on artificial intelligence*, volume 35, 3208–3216.

Zareian, A.; Karaman, S.; and Chang, S.-F. 2020. Bridging knowledge graphs to generate scene graphs. In *Computer Vision–ECCV 2020: 16th European Conference, Glasgow, UK, August 23–28, 2020, Proceedings, Part XXIII 16*, 606–623. Springer.

The following sections provide detailed information about the datasets and the training process for each scenario in our experiments. Additionally, we present further analysis through ablation experiments.

### Dataset Settings

Detailed descriptions of the used datasets are provided in this section.

#### Road Sign:

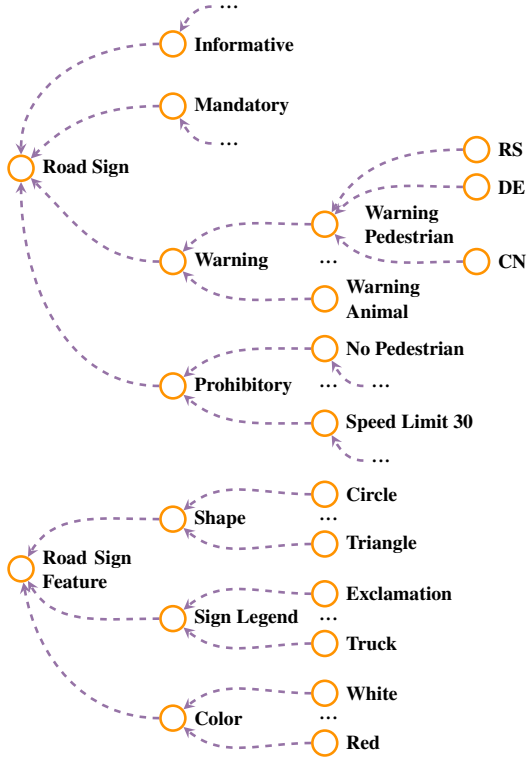


Figure 4: An abstract of hierarchical relations existing in the road sign recognition domain.

We leverage three commonly used road sign recognition datasets to evaluate our model. They are the German Traffic Sign Recognition Benchmark (GTSRB) from Stallkamp et al. (2011), Chinese Traffic Sign Dataset (CTSD) from Yang et al. (2015), and Russian Traffic Sign Images Dataset (RTSD) from Shakhuro and Konouchine (2016). The detailed information on these three datasets and the synthetic images of road sign elements are listed in Table 10 and Table 11. The hierarchical relations are shown in Figure 4.

#### DVM-CAR:

Deep Visual Marketing Car (DVM-CAR) dataset (Huang et al. 2021) is created from 335,562 used car advertisements. It contains 1,451,784 images of cars from various angles, as well as their sales and technical data. We use this dataset to predict the car model from the given images. All images are resized to the resolution of  $128 \times 128$ . We use the same

Dataset	Total Images	Road Sign Classes
GTSRB	51970	43
CTSD	6164	58
RTSD	32983	64

Table 10: GTSRB, CTSD, and RTSD represent three road sign recognition datasets of China, Germany, and Russia. The total images and class numbers are listed in the table.

Feature Types	Sub-class	Image	Sub-class	Image
Color	Black		Blue	
	Brown		Green	
	Red		White	
	Yellow			
Shape	Circle		Diamond	
	Octagon		Triangle-Down	
	Triangle-Up			
Sign Legend	Animal		Bicycle	
	Exclamation		Person	
	Sand		SnowFlake	
	Truck		TwoPerson	
	Vehicle			

Table 11: Synthetic Images in the Road Sign Recognition Domain. Seven colors, five shapes, and nine sign legends are included. For each type, we generated synthetic images as illustrated in the table.

training, validation, and testing setting as MMCL (Hager, Menten, and Rueckert 2023). Their dataset consists of 286 classes with a total of 418,100 training samples, 104,308 validation samples, and 525,557 testing samples. Samples of synthetic images used for training can be seen in Table 12. We generate 20 pure color images with small variations for each color category. For each body type category, we collect 20 sketch images. Note that we extract the image instance-level triplets from the tabular annotations provided in the DVM-CAR dataset. Figure 5 shows an abstract of relations between one sample image instance and the other nodes in the KG.






Feature Types	Sub-class	Image	Sub-class	Image
Color	Beige		Black	
	Blue		Bronze	
	Brown		Burgundy	
	Gold		Green	
	Grey		Indigo	
	Magenta		Maroon	
	Navy		Orange	
	Pink		Purple	
	Red		Silver	
	Turquoise		White	
	Yellow			
Bodytype	Convertible		Coupe	
	Estate		Hatchback	
	Limousine		Minibus	
	MPV		Pickup	
	Saloon		SUV	
	Van			

Table 12: Synthetic Images in the Car Recognition Domain. Twenty-one colors and eleven body type sketches are included. We generate synthetic images for each color and collect body type sketches on the internet.

### ImageNet:

Mini-ImageNet (Vinyals et al. 2016) is a subset of the ImageNet dataset, consisting of 60K images of size  $84 \times 84$  with 100 classes, each having 600 examples. ImageNet-Skeeth (Wang et al. 2019) comprises 50000 images, 50 images for each of the 1000 ImageNet classes. Here, we collect the 100 classes in mini-ImageNet from 1000 classes of ImageNet-Sketch for training. We employ three distinct datasets for our evaluation: ImageNetV2 (Recht et al. 2019), ImageNet-R (Hendrycks et al. 2021a), and ImageNet-A (Hendrycks et al. 2021b). ImageNetV2 comprises 10 fresh test images for each class, sharing the same set of labels as mini-ImageNet. ImageNet-R includes various artistic representations such as art, cartoons, and deviant styles, covering 200 classes from ImageNet. Lastly, ImageNet-A features unaltered, real-world examples that occur naturally. For our purposes, we assess only those

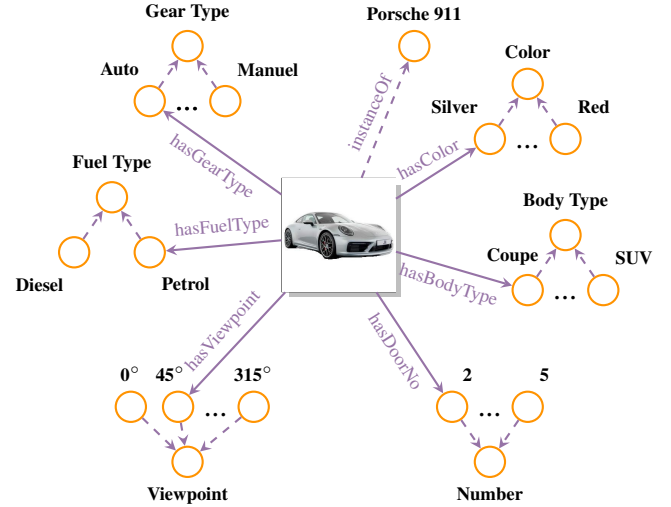


Figure 5: The relations between one image instance of Porsche 911 with other nodes in the car recognition KG.

classes that overlap with mini-ImageNet. An abstract of hierarchical relations extracted from the WordNet in the ImageNet Domain is illustrated in Figure 6.

### Training Details

Our baseline ResNet50 has a simple structure of a ResNet50 backbone as an encoder and full connect layers as a decoder. The ResNet50 backbone is untrained and randomly initialized in a Xavier manner. Our KGV model and the other baselines, GCNZ and DGP, use the same image encoder backbone. The node and relation lookup tables, which contain the embeddings of nodes and relations in the knowledge graph, are also initialized, following the initialization method proposed in transE (Bordes et al. 2013). The relation, represented as ‘sub class of/instance of’ is an exception. It is initialized with a vector of all zeros and frozen during the training procedure. We use one NVIDIA A100 GPU with 80GB memory to train the models. Each algorithm is run with three random seeds to get the average performance.

The hyperparameters used in the three domains are illustrated as follows:

- **Road Sign Recognition Domain:** The weight balance  $\beta$  defined is 0.1. We train the baseline and our model with the Adam optimizer and a constant learning rate of 0.0002. The total training epochs are 120. The mini-batch size is 32. We resize all the input images to  $32 \times 32$ .
- **Car Recognition Domain:** We resize all input image to  $128 \times 128$ . The batch size we select is 512. Adam optimizer with a learning rate of 0.001 and cosines annealing learning rate schedule is utilized for optimization. The training epochs for 5%, 10%, 50%, and 100% of data are 600, 200, 150, and 100, respectively. The balance  $\beta$  we use is 0.5.
- **ImageNet Domain:** Both Baseline and our model KGV

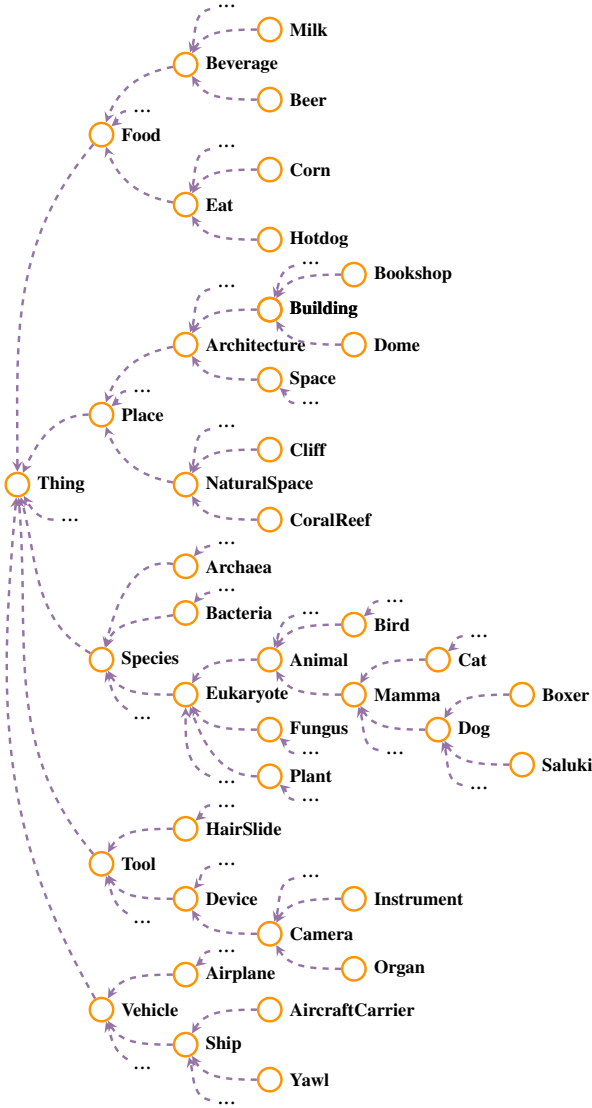


Figure 6: An abstract of the hierarchical relations existing in the ImageNet domain.

are trained with Adam optimizer and a learning rate of 0.001. The batch size we select is 1024 and the training epoch is 150. We resize all the input images to  $84 \times 84$ . The balance  $\beta$  we use is 0.5.

### Additional Analysis

In this section, we further analyze which knowledge plays the most important role in the performance.

#### ImageNet:

As demonstrated in Table 13, we performed ablation studies on our KGV method by excluding either prior knowledge of color or sketch. Our results indicate that knowledge of color significantly impacts performance on the Mini-ImageNet, ImageNetV2, and ImageNet-A datasets. The knowledge of sketch proves to be more critical for classifying the

Model	KGV	KGV w/o color	KGV w/o sketch
Mini-ImageNet	<b>66.8%</b>	63.6% +3.2%	64.4% +2.4%
ImageNetV2	<b>52.7%</b>	50.0% +2.7%	51.5% +1.2%
ImageNet-R	<b>41.4%</b>	39.5% +1.9%	29.7% +11.7%
ImageNet-A	<b>6.8%</b>	5.1% +1.7%	6.2% +0.6%

Table 13: Classification Accuracy in the ImageNet Domain.

ImageNet-R dataset, likely due to the similarity between the ImageNet-Sketch and ImageNet-R datasets.